Anh Tran (SNL); Julien Tranchida (CEA Cadarache)

Multi-fidelity Gaussian process and Bayesian optimization for materials design: Application to ternary random alloys

Sandia National Laboratories is a multimission laboratory managed and operated by National Technology and Engineering Solutions of Sandia, LLC., a wholly owned subsidiary of Honeywell International, Inc., for the U.S. Department of Energy's National Nuclear Security Administration under contract DE-NA-0003525. The views expressed in the article do not necessarily represent the views of the U.S. Department of Energy or the United States Government.

Tran, A., Tranchida, J., Wildey, T., & Thompson, A. P. (2020). Multi-fidelity machine-learning with uncertainty quantification and Bayesian optimization for materials design: Application to ternary random alloys. The Journal of Chemical Physics, 153(7), 074705.

The problem we are trying to solve

High entropy alloys

- Random alloys with four or more principal components.
- HEAs are promising materials (**refractory** and aerospace applications, **nuclear degradation-resistant** materials, …).
- At Sandia, HEAs are manufactured by **additive manufacturing** techniques.
- Prototypical compositions: FeCoCrMnNi, MoNbTaW.

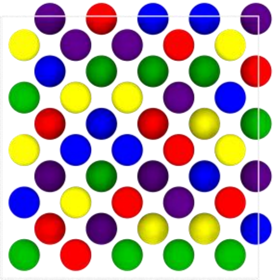

Materials design problem

- Materials design can be seen as an inverse problem in the structure-property relationship.
- In the context of modern random alloys, optimizing functional performances requires the exploration of vast composition spaces.
- The developed ML approaches will be applied to exploring functional properties of different alloy compositions: AlNbTi, MoNbTaW, ...
- Comparisons to experimental measurements of additive manufacturing based HEAs performed at Sandia will allow to probe our methods.

The problem we are trying to solve

High entropy alloys

- Random alloys with four or more principal components.
- HEAs are promising materials (**refractory** and aerospace applications, **nuclear degradation-resistant** materials, …).
- At Sandia, HEAs are manufactured by **additive manufacturing** techniques.
- Prototypical compositions: FeCoCrMnNi, MoNbTaW.

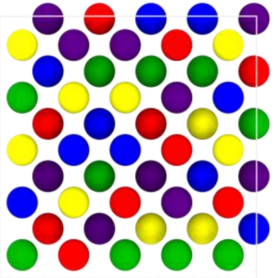

Machine-learning problem

- The predicting capabilities of high-accuracy first-principles methods, such as Density Functional Theory (DFT) is limited by their computational cost.
- Machine-Learning interatomic potentials (ML-IAP) are emerging as a promising solution to reduce this cost while preserving accuracy.
- However, the use of DFT and ML-IAP remains mostly segregated.
- We leverage Gaussian process and Bayesian optimization to fuse the predictions of DFT and ML-IAP, and develop a multi-fidelity framework for random alloys. We use it to accurately and efficiently predict materials properties.

SNAP potential for ternary random alloy

- A framework was developed to generate a DB for ternary composition.

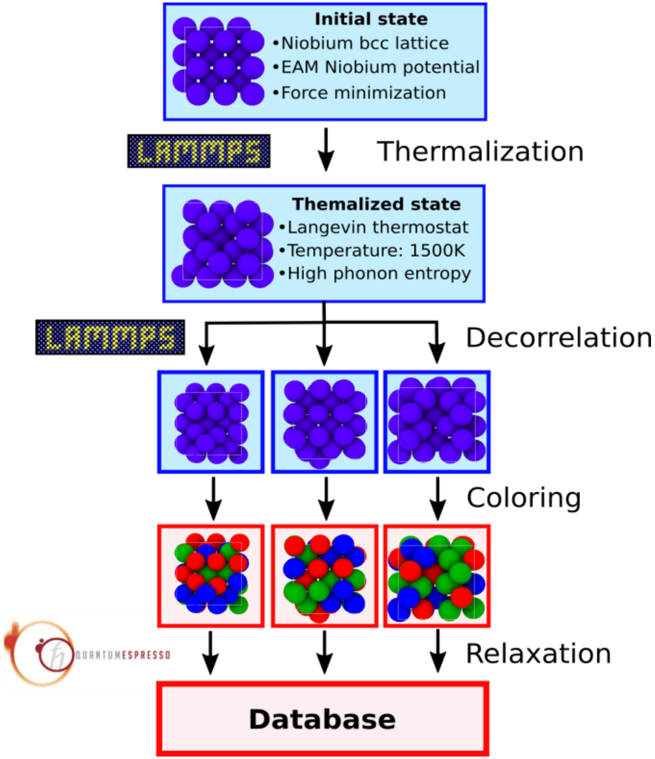

Initial state
- Niobium bcc lattice
- EAM Niobium potential
- Force minimization

Thermalization

Themalized state
- Langevin thermostat
- Temperature: 1500K
- High phonon entropy

Decorrelation

Coloring

Relaxation

Database

- Generated SNAP training set:

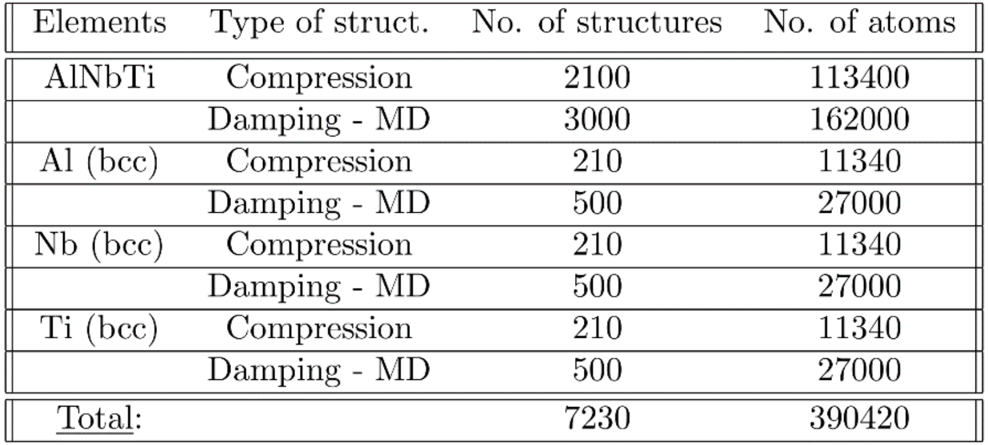

Elements	Type of struct.	No. of structures	No. of atoms
AlNbTi	Compression	2100	113400
	Damping - MD	3000	162000
Al (bcc)	Compression	210	11340
	Damping - MD	500	27000
Nb (bcc)	Compression	210	11340
	Damping - MD	500	27000
Ti (bcc)	Compression	210	11340
	Damping - MD	500	27000
Total:		7230	390420

- “Large” but unbalanced dataset: a lot of atomic configurations, but mainly at equicomposition.

- We only work on bcc structures.

SNAP potential for ternary random alloy

- A framework was developed to generate a DB for ternary composition.

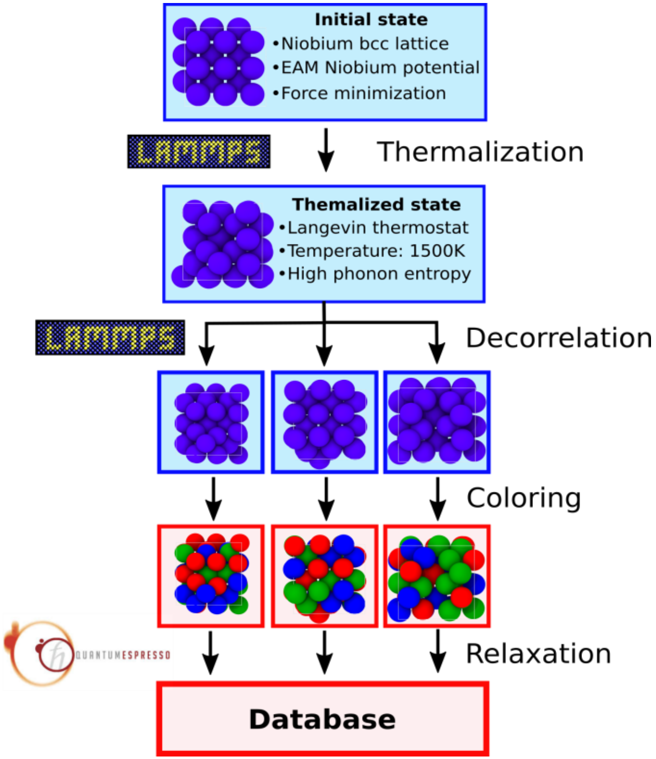

Initial state
- Niobium bcc lattice
- EAM Niobium potential
- Force minimization

LAMMPS Thermalization

Themalized state
- Langevin thermostat
- Temperature: 1500K
- High phonon entropy

LAMMPS Decorrelation

Coloring

QUANTUMESPRESSO Relaxation

Database

- SNAP - Dakota machinery:

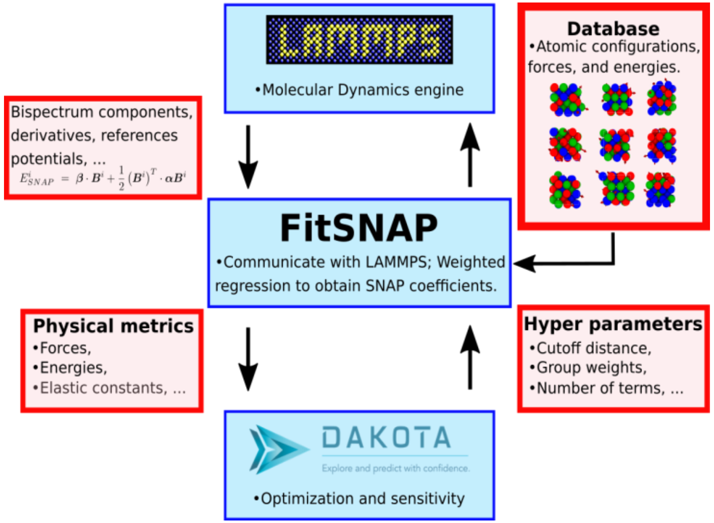

LAMMPS
- Molecular Dynamics engine

Database
- Atomic configurations, forces, and energies.

Bispectrum components, derivatives, references potentials, ...

$E^i_{SNAP} = \beta \cdot B^i + \frac{1}{2}(B^i)^T \cdot \alpha B^i$

FitSNAP
- Communicate with LAMMPS; Weighted regression to obtain SNAP coefficients.

Physical metrics
- Forces,
- Energies,
- Elastic constants, ...

Hyper parameters
- Cutoff distance,
- Group weights,
- Number of terms, ...

DAKOTA

Explore and predict with confidence.

- Optimization and sensitivity

- A SNAP IAP for AlNbTi was trained on the generated training set.

Thompson, A. P., *et al*.. (2015). J. Comp. Phys., 285, 316-330.

Focus on one property: the bulk modulus

- The data consists of **High-** and **Low-fidelity bulk modulus** calculations accros the AlNbTi composition space.
- We leveraged two atomistic approaches:

Ab initio calculations

- We used density-functional theory as implemented in Quantum Espresso.
- Slow calculations, but accurate for materials design.
- **High-Fidelity (HF) Data**

Classical potential calculations

- We used LAMMPS and a Machine Learning SNAP interatomic potential.
- Orders of magnitude faster than HF, but less accurate for materials design.
- **Low-Fidelity (LF) Data**

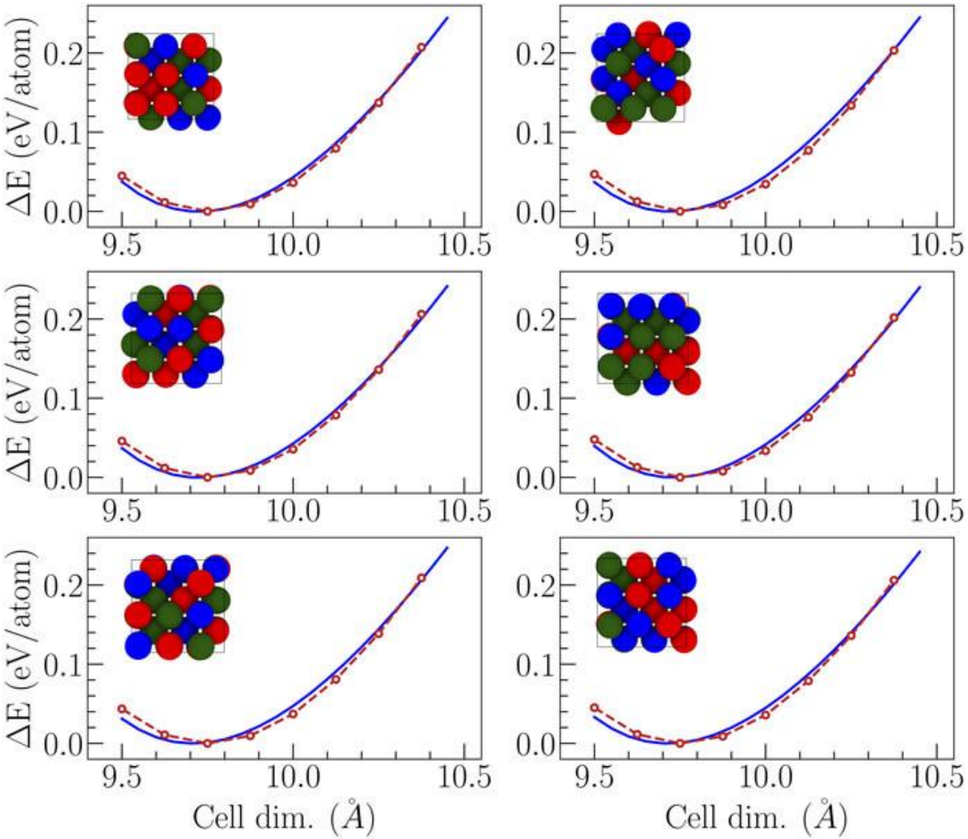

Focus on one property: the bulk modulus

- For each composition across the AlNbTi diagram, Equation of State (EOS) calculations are performed. Their fitting (Birch-Murnaghan polynomials) allows to extract the bulk modulus:

$$E(V) = E_0 + \frac{9V_0B_0}{16}\left\{B_0'\left[\left(\frac{V_0}{V}\right)^{\frac{3}{2}}-1\right]^3 + \left[\left(\frac{V_0}{V}\right)^{\frac{3}{2}}-1\right]^2\left[6-4\left(\frac{V_0}{V}\right)^{\frac{3}{2}}\right]\right\}$$

HF bulk modulus predictions

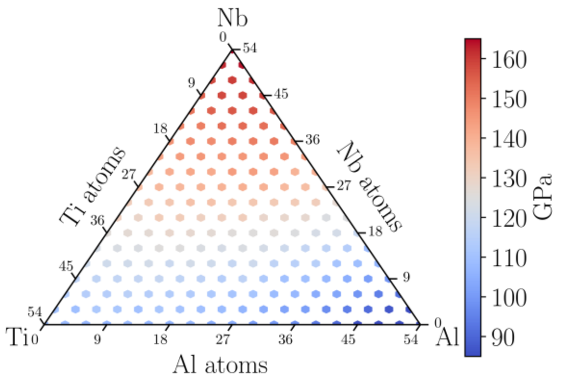

LF bulk modulus predictions

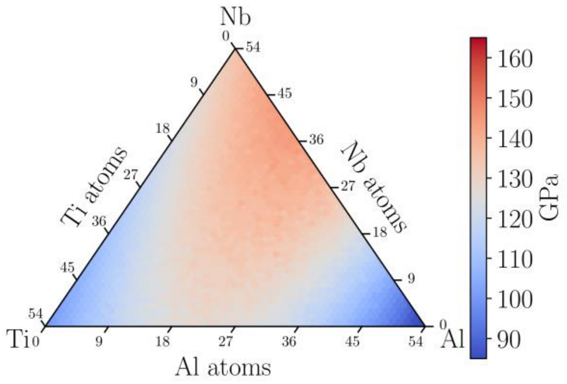

- This HF and LF data is used as a training and testing set for the Gaussian process model.

Gaussian process - Introduction

- A powerful and flexible framework
- And versatile, but in what sense?
  - Multi-objective
  - Multi-task
  - Multi-fidelity
  - Mixed-integer
  - Scalable for Big Data
  - High-dimensional
  - Asynchronous parallel
  - And more
- An animation of Bayesian optimization

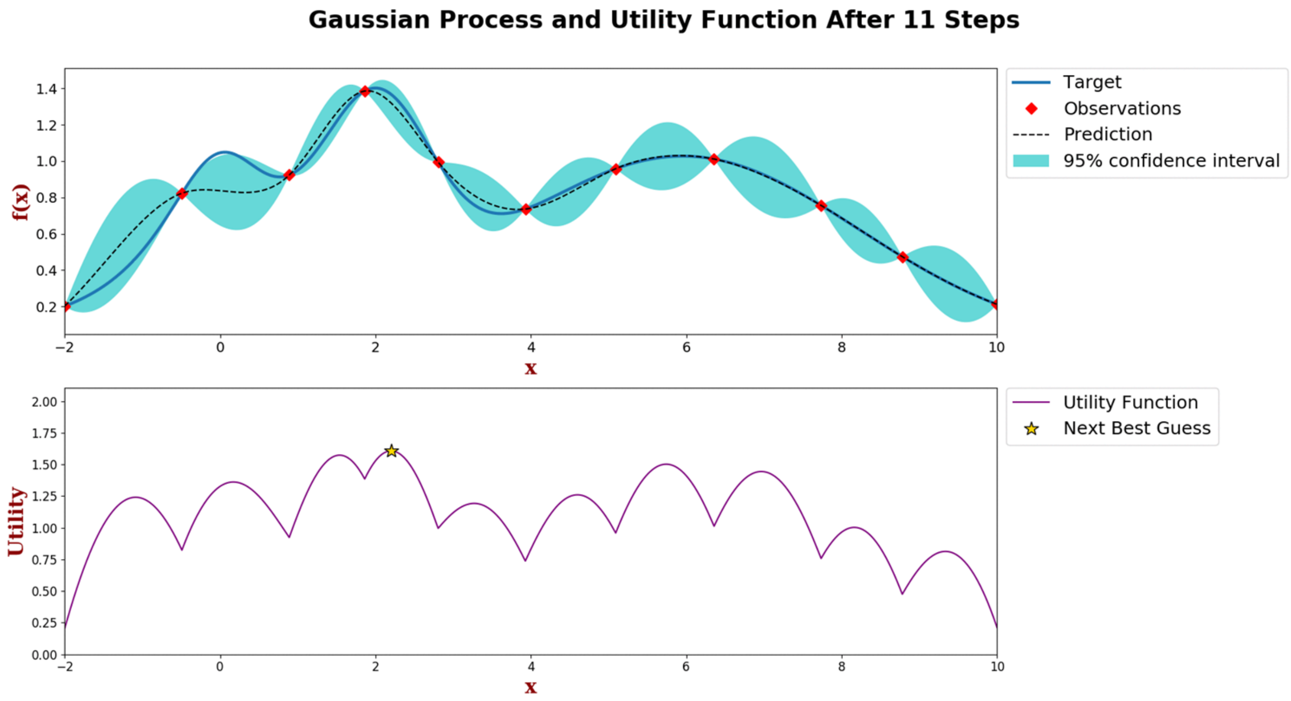

Gaussian process - Introduction

- Let $\mathcal{D}_n = \{\mathbf{x}_i, y_i\}_{i=1}^n$ denote the set of observations
- $\mathbf{x}$ denote an arbitrary test points

- Prediction is a Gaussian distribution

$$\mu_n(\mathbf{x}) = \mu_0(\mathbf{x}) + \mathbf{k}(\mathbf{x})^T(\mathbf{K} + \sigma^2\mathbf{I})^{-1}(\mathbf{y} - \mathbf{m})$$

$$\sigma_n^2(\mathbf{x}) = k(\mathbf{x}, \mathbf{x}) - \mathbf{k}(\mathbf{x})^T(\mathbf{K} + \sigma^2\mathbf{I})^{-1}\mathbf{k}(\mathbf{x})$$

- $\mathbf{k}(\mathbf{x})$ is a vector of covariance terms.

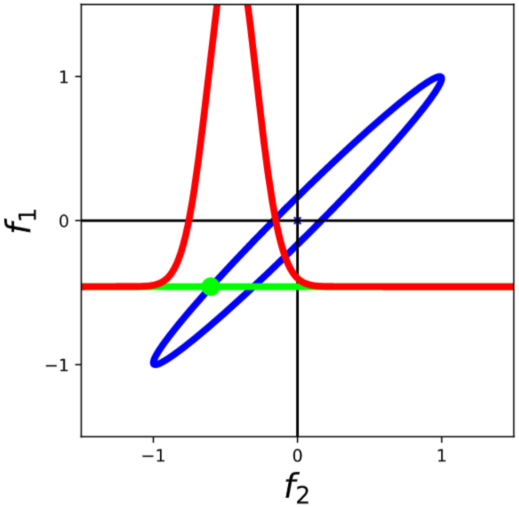

A conditional of a Gaussian is Gaussian.
Photo courtesy of Neil Lawrence.
http://inverseprobability.com/talks/notes/gaussian-processes.html

[2] If $P(\mathbf{f},\mathbf{g}) = \mathcal{N}\left(\begin{bmatrix} a \\ b \end{bmatrix}, \begin{bmatrix} A & C \\ C^\top & B \end{bmatrix}\right)$ then $P(\mathbf{f}|\mathbf{g}) = \mathcal{N}(a + CB^{-1}(y - b), A - CB^{-1}C^\top)$ (cf. Appendix A [29]).

Gaussian process - Introduction

- Kernels: $\mathbf{K} \in \mathbb{R}^{n \times n}$
  - Stationary (default)

    $$\mathbf{K}_{ij} = k(\mathbf{x}_i, \mathbf{x}_j) = k(\mathbf{x}_j, \mathbf{x}_i) = \mathbf{K}_{ji}$$

  - Anisotropic vs. isotropic
  - Symmetric positive semi-definite matrix
  - Many good choices
  - Affect smoothness of GP
  - (hint: first derivative at origin)

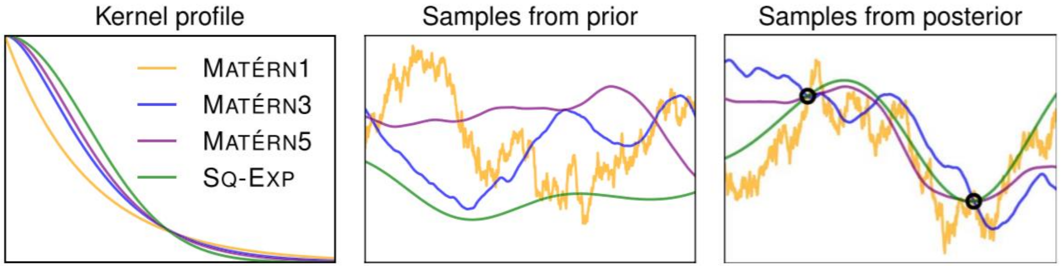

B. Shahriari, K. Swersky, Z. Wang, R. P. Adams, and N. de Freitas, Proc. IEEE 104, 148 (2016).

$$k_{\text{Matérn1}}(\mathbf{x}, \mathbf{x}') = \theta_0^2 \exp(-r)$$

$$k_{\text{Matérn3}}(\mathbf{x}, \mathbf{x}') = \theta_0^2 \exp(-\sqrt{3}r)(1 + \sqrt{3}r)$$

$$k_{\text{Matérn5}}(\mathbf{x}, \mathbf{x}') = \theta_0^2 \exp(-\sqrt{5}r)\left(1 + \sqrt{5}r + \tfrac{5}{3}r^2\right)$$

$$k_{\text{sq-exp}}(\mathbf{x}, \mathbf{x}') = \theta_0^2 \exp\left(-\tfrac{1}{2}r^2\right)$$

Gaussian process - Introduction

- How to train a GP
  - Maximizing the log marginal likelihood function

$$\begin{aligned}\log p(\mathbf{y}|\mathbf{x}_{1:n},\theta) \quad = \quad & -\tfrac{n}{2}\log(2\pi) - \tfrac{1}{2}\log|\mathbf{K}^{\theta}+\sigma^2\mathbf{I}| \\ & -\tfrac{1}{2}(\mathbf{y}-\mathbf{m}_{\theta})^{T}(\mathbf{K}^{\theta}+\sigma^2\mathbf{I})^{-1}(\mathbf{y}-\mathbf{m}_{\theta})\end{aligned}$$

  - Alternatively, can treat hyper-parameters as stochastic parameters and marginalize out using MC

Snoek, J., Larochelle, H., & Adams, R. P. (2012). Practical bayesian optimization of machine learning algorithms. Advances in neural information processing systems, 25.

- Complexity $\mathbf{K}^{-1} \rightarrow \mathcal{O}(n^3)$
- More computationally expensive with more data
- Approximations are available to reduce complexity at the cost of accuracy, e.g. low-rank approx.

Gaussian process - Introduction

- What is the point of optimization?
  - Everything is about efficiency
  - Crux: how to select the next input parameters
  - Debate of optimization policies
- Bayesian optimization is a gradient-free approach
- Next input parameters are found by maximizing acquisition function
- Active learning: balancing exploration vs. exploitation
- Minimal dataset

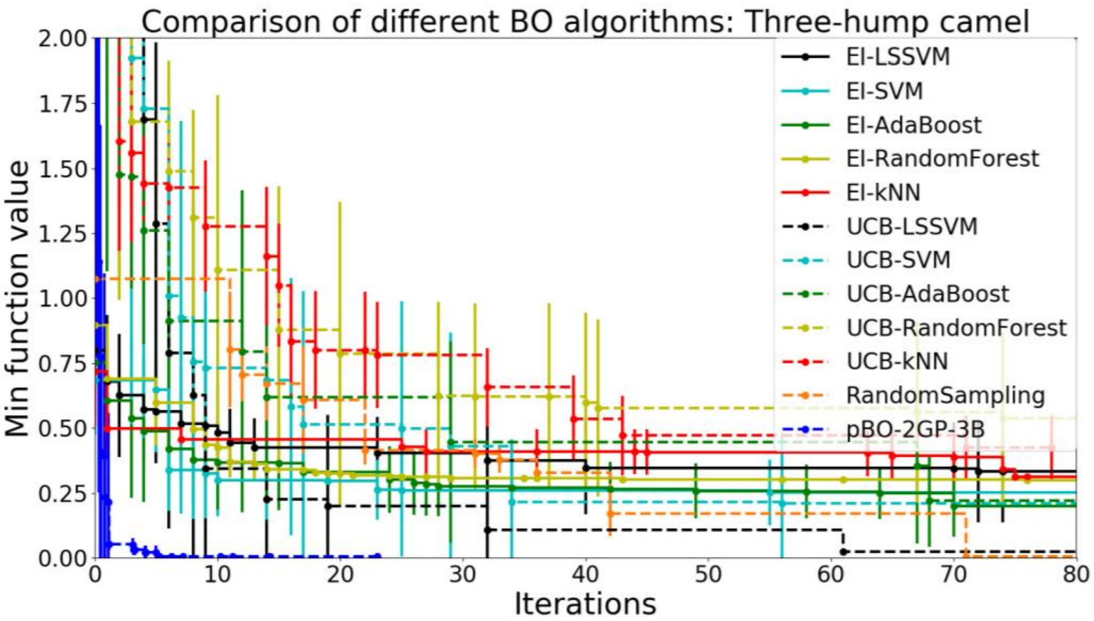

Gaussian process - Introduction

- Acquisition function

$$\gamma(\mathbf{x}) = \frac{\mu(\mathbf{x}; \{\mathbf{x}_i, y_i\}_{i=1}^{n}, \theta) - f(\mathbf{x}_{\text{best}})}{\sigma(\mathbf{x}; \{\mathbf{x}_i, y_i\}_{i=1}^{n}, \theta)}$$

- Probability of improvement (PI)

$$a_{\text{PI}}(\mathbf{x}; \{\mathbf{x}_i, y_i\}_{i=1}^{n}, \theta) = \Phi(\gamma(\mathbf{x}))$$

Mockus, Jonas (1975). “On Bayesian methods for seeking the extremum”. In: Optimization Techniques IFIP Technical Conference. Springer, pp. 400–404.
Mockus, Jonas (1982). “The Bayesian approach to global optimization”. In: System Modeling and Optimization, pp. 473–481

- Expected improvement (EI)

$$a_{\text{EI}}(\mathbf{x}; \{\mathbf{x}_i, y_i\}_{i=1}^{n}, \theta) = \sigma(\mathbf{x}; \{\mathbf{x}_i, y_i\}_{i=1}^{n}, \theta) \cdot (\gamma(\mathbf{x})\Phi(\gamma(\mathbf{x})) + \phi(\gamma(\mathbf{x}))$$

- Upper confidence bound (UCB)

$$a_{\text{UCB}}(\mathbf{x}; \{\mathbf{x}_i, y_i\}_{i=1}^{n}, \theta) = \mu(\mathbf{x}; \{\mathbf{x}_i, y_i\}_{i=1}^{n}, \theta) + \kappa\sigma(\mathbf{x}; \{\mathbf{x}_i, y_i\}_{i=1}^{n}, \theta)$$

Srinivas, Niranjan et al. (2009). “Gaussian process optimization in the bandit setting: No regret and experimental design”. In: arXiv preprint arXiv:0912.3995.
Srinivas, Niranjan et al. (2012). “Information-theoretic regret bounds for Gaussian process optimization in the bandit setting”. In: IEEE Transactions on Information Theory 58.5, pp. 3250–3265.

Gaussian process - Multi-fidelity

- Auto-regressive formulation $f_H(\boldsymbol{x}) = \rho f_L(\boldsymbol{x}) + \delta(\boldsymbol{x})$
- Covariance matrix

$$\tilde{\boldsymbol{K}} = \begin{pmatrix} \sigma_L^2 \boldsymbol{K}_L(\boldsymbol{x}_L, \boldsymbol{x}_L) & \rho\sigma_L^2 \boldsymbol{K}_L(\boldsymbol{x}_L, \boldsymbol{x}_H) \\ \rho\sigma_L^2 \boldsymbol{K}_L(\boldsymbol{x}_H, \boldsymbol{x}_L) & \rho^2\sigma_L^2 \boldsymbol{K}_L(\boldsymbol{x}_H, \boldsymbol{x}_H) + \sigma_d^2 \boldsymbol{K}_D(\boldsymbol{x}_H, \boldsymbol{x}_H) \end{pmatrix}$$

- Posterior mean

$$\mu(\boldsymbol{x}) \quad = \quad \mu_0(\boldsymbol{x}) + \tilde{\boldsymbol{k}}(\boldsymbol{x})^T (\tilde{\boldsymbol{K}} + \sigma^2 \boldsymbol{I})^{-1} (\tilde{\boldsymbol{y}} - \tilde{\boldsymbol{m}})$$

- Posterior variance

$$\begin{aligned} \sigma^2(\boldsymbol{x}) &= \rho^2 \sigma_L^2(\boldsymbol{x}) + \sigma_d^2(\boldsymbol{x}) \\ &\quad - \tilde{\boldsymbol{k}}(\boldsymbol{x})(\tilde{\boldsymbol{K}} + \sigma^2 \boldsymbol{I})^{-1} \tilde{\boldsymbol{k}}(\boldsymbol{x}) \end{aligned}$$

- Log marginal likelihood

$$\begin{aligned} & \log p(\tilde{\boldsymbol{y}} | \boldsymbol{x}_{1:n_L}, \boldsymbol{x}_{1:n_H}, \tilde{\theta}) \\ = & -\frac{1}{2}(\tilde{\boldsymbol{y}} - \tilde{\boldsymbol{m}})^T (\tilde{\boldsymbol{K}}^{\tilde{\theta}} + \sigma^2 \boldsymbol{I})^{-1} (\tilde{\boldsymbol{y}} - \tilde{\boldsymbol{m}}) \\ & -\frac{1}{2} \log |\tilde{\boldsymbol{K}}^{\tilde{\theta}} + \sigma^2 \boldsymbol{I}| - \frac{n_H + n_L}{2} \log(2\pi) \end{aligned}$$

- Fidelity level to query

$$t^* = \operatorname*{argmin}_t \left(C_t \int_{\mathcal{X}} \sigma^2(\boldsymbol{x}) d\boldsymbol{x} \right)$$

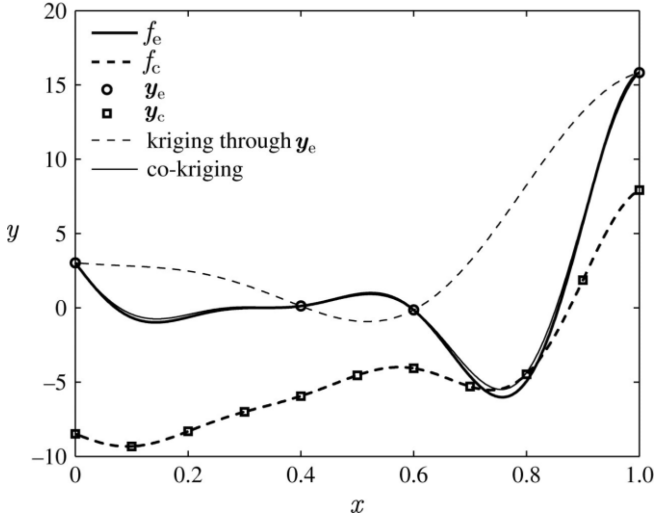

Photo courtesy of Forrester (2007).

1. Kennedy, Marc C and Anthony O'Hagan (2000). "Predicting the output from a complex computer code when fast approximations are available". In: Biometrika 87.1, pp. 1–13
2. Yang, X., Zhu, X., & Li, J. (2020). When bifidelity meets cokriging: An efficient physics-informed multifidelity method. SIAM Journal on Scientific Computing, 42(1), A220-A249.
3. Xiao, M., Zhang, G., Breitkopf, P., Villon, P., & Zhang, W. (2018). Extended Co-Kriging interpolation method based on multi-fidelity data. Applied Mathematics and Computation, 323, 120-131.
4. Tran, A., Wildey, T., & McCann, S. (2020). sMF-BO-2CoGP: A sequential multi-fidelity constrained Bayesian optimization framework for design applications. Journal of Computing and Information Science in Engineering, 20(3).
5. Forrester, A. I., Sóbester, A., & Keane, A. J. (2007). Multi-fidelity optimization via surrogate modelling. Proceedings of the royal society a: mathematical, physical and engineering sciences, 463(2088), 3251-3269.

A multi-scale perspective

- But try to look at this from a multi-fidelity perspective
- Machine learning prediction is not very accurate, but computationally cheap
- DFT is accurate, but expensive
- Propose a multi-fidelity approach to support ML prediction with DFT when it's necessary.

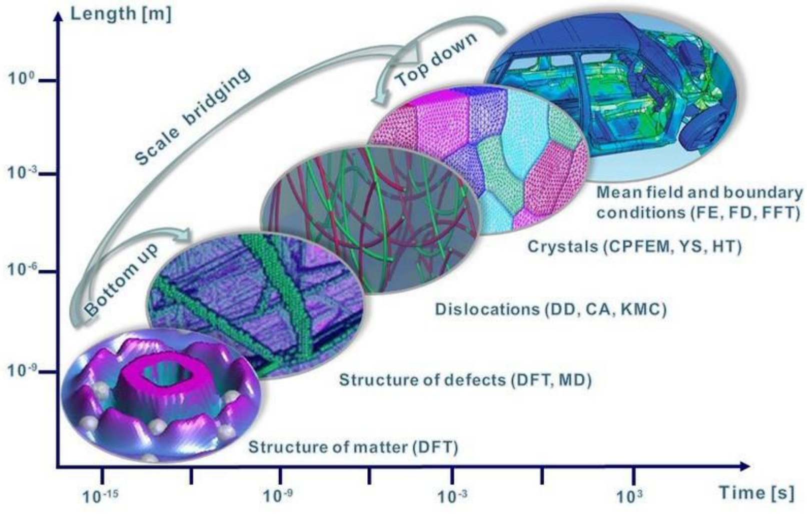

Photo courtesy of Dierk Raabe. http://www.dierk-raabe.com/multiscale-modeling/

Multi-fidelity for multi-scale

- Materials design: inverse problem
- From chemical composition to materials properties

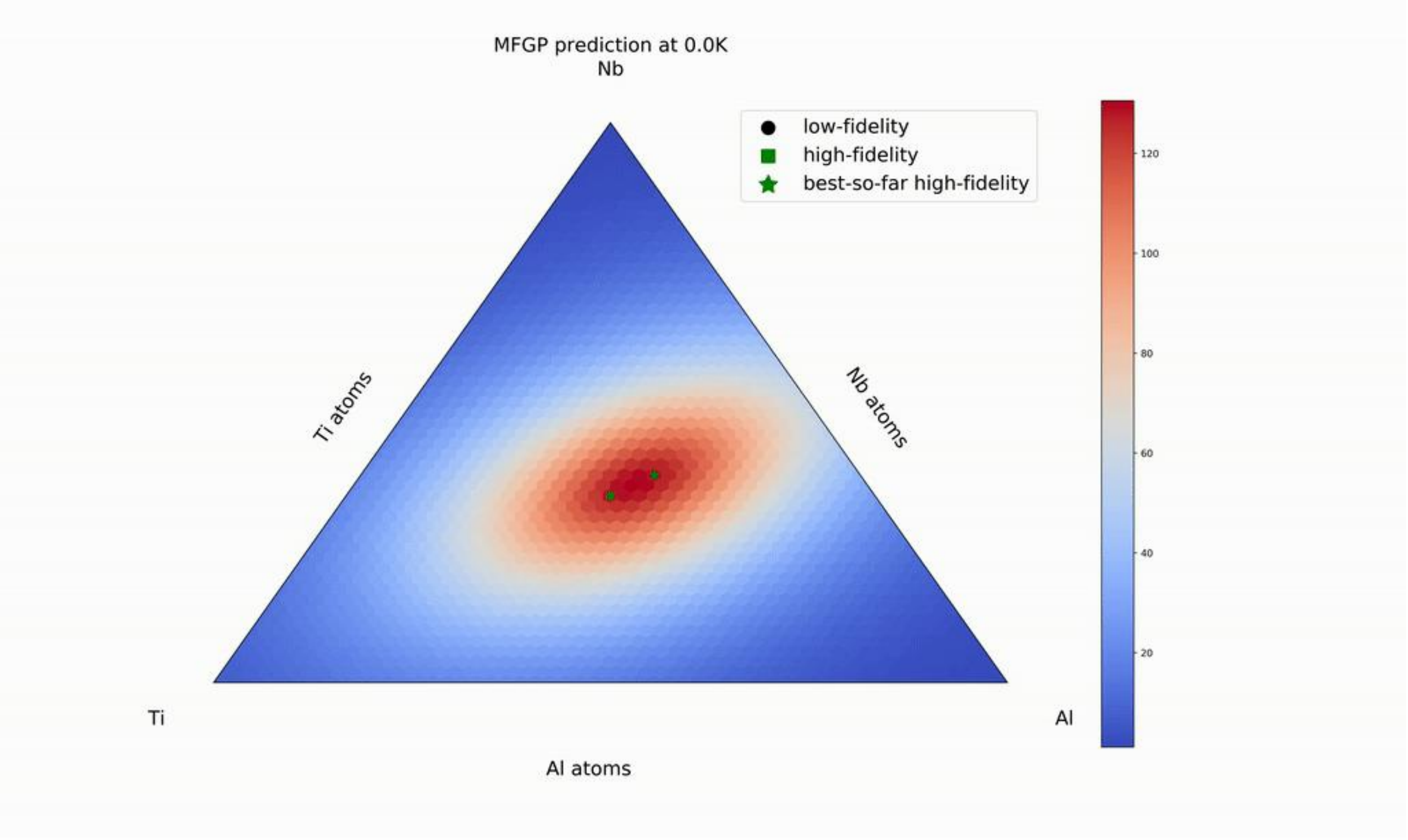

Bayesian Optimization Parallelism

- A MPI perspective: Why parallelize optimization?

arguments:

- focus on multi-core HPC architecture and expensive, high-fidelity simulations
- **Amdahl's law**: diminishing returns, i.e. rewards for parallelizing solvers diminish as # of processors increase
- **motivation**: can we search for the optimal point in **faster** wall-clock time, assuming HPC power is sufficient and/or abundant?
- obviously **beneficial** when computing resource is **sufficient**

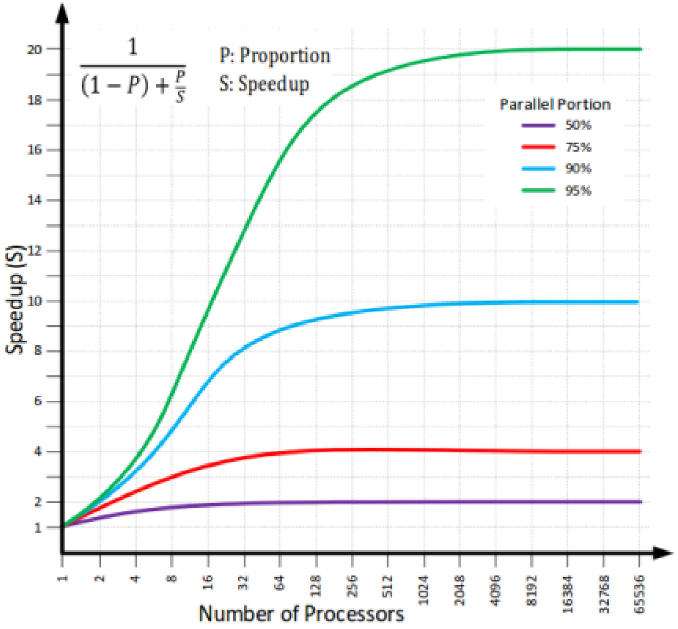

Figure 19: Amdahl's law for parallelization.

Bayesian Optimization Parallelism

- A MPI perspective: Why parallelize optimization?

  might as well be **beneficial** when computing resource is **insufficient**; examples:

  - $P = 0.95 \rightarrow$ SpeedUp $\approx$ 20 times
  - MD simulation takes 3 hours to finish with 256 procs → **20 cases**/60 hours
  - or 60 hours (2.5 days) with 1 proc for 1 case → **256 cases**/60 hours
  - **fixed** computational budget: 256 ×60 CPU hours
  - **question:** in the period of **2.5 days**, are we better off with **20 sequential** runs, or with **256 batch-parallel** runs? what about 5 days (**40 vs. 512**)? 10 days (**80 vs. 1024**)? asymptotically?

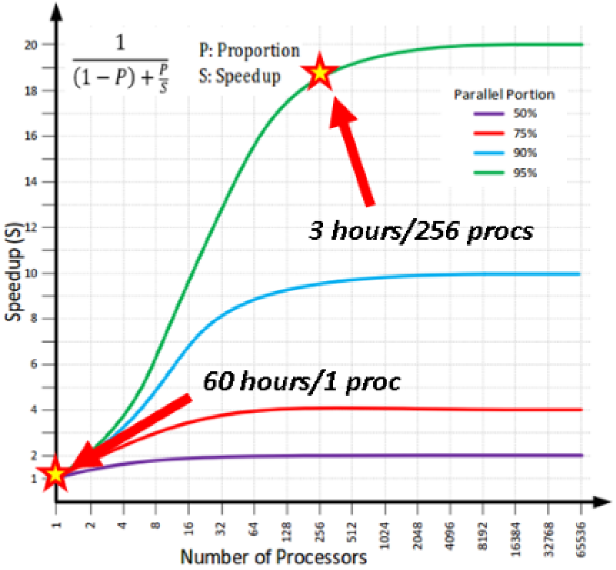

Figure 20: Amdahl's law for parallelization.

Bayesian Optimization Parallelism

- A MPI perspective
- Why asynchronous parallel?

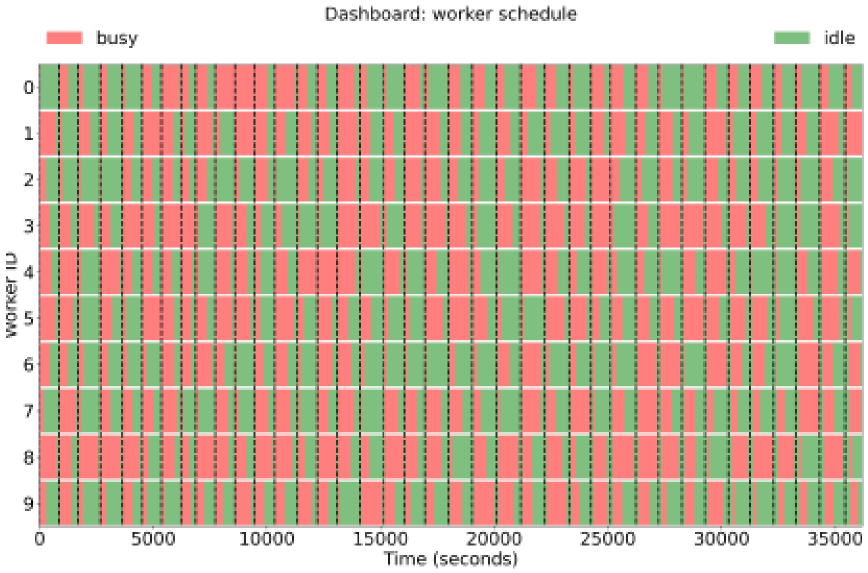

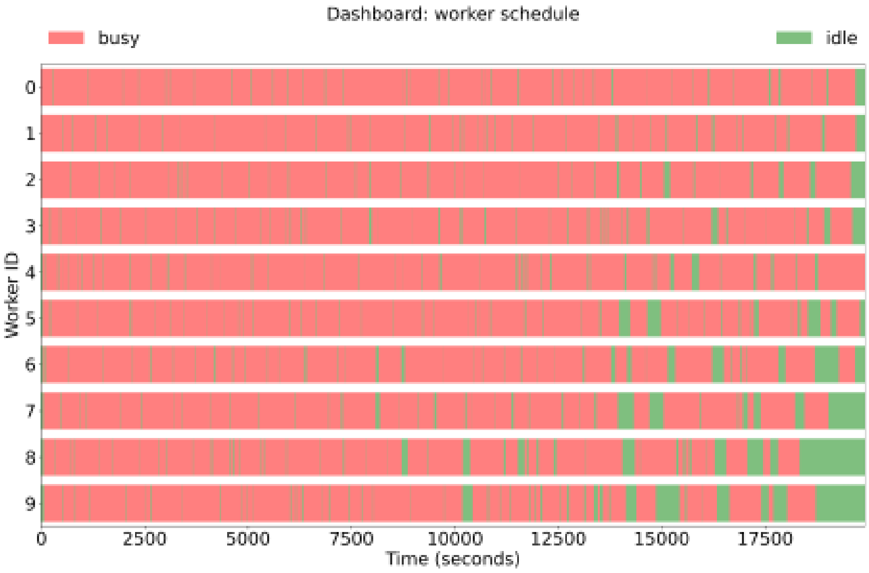

The code, the data, and the tutorials

- https://dakota.sandia.gov/
- Source code available: https://dakota.sandia.gov/download.html
- A Sandia National Laboratories’s flagship software in uncertainty quantification and optimization
- How to compile Dakota on Ubuntu 20.04 LTS: https://dakota.sandia.gov/content/linux-ubuntu-2004

```
apt-get install gcc g++ gfortran cmake libboost-
all-dev libblas-dev liblapack-dev libopenmpi-dev
openmpi-bin gsl-bin libgsl-dev python perl
libhdf5-dev

cmake \
-D CMAKE_C_FLAGS="-O2" \
-D CMAKE_CXX_FLAGS="-O2" \
-D CMAKE_Fortran_FLAGS="-O2“ \
-D DAKOTA_HAVE_GSL:BOOL=TRUE \
-D HAVE_QUESO:BOOL=TRUE \
-D DAKOTA_HAVE_MPI:BOOL=TRUE \
-D DAKOTA_HDF5:BOOL=TRUE \
-D Boost_NO_BOOST_CMAKE:BOOL=TRUE\
 ${DAK_SRC}
```

The code, the data, and the tutorials

- https://dakota.sandia.gov/content/manuals
- Interface examples: **src/dakota-examples/official/drivers/**
- Directory
- Two pseudo-simulations
  - **snap_query.py**
  - **dft_query.py**
- Input: **params.in**
- Output: **results.out**
- I/O interface (direct interface with Python also available)
- Dakota input file: **dakota_dft.in**
- **https://github.com/anhvt2/psi-k-tutorials-2021**

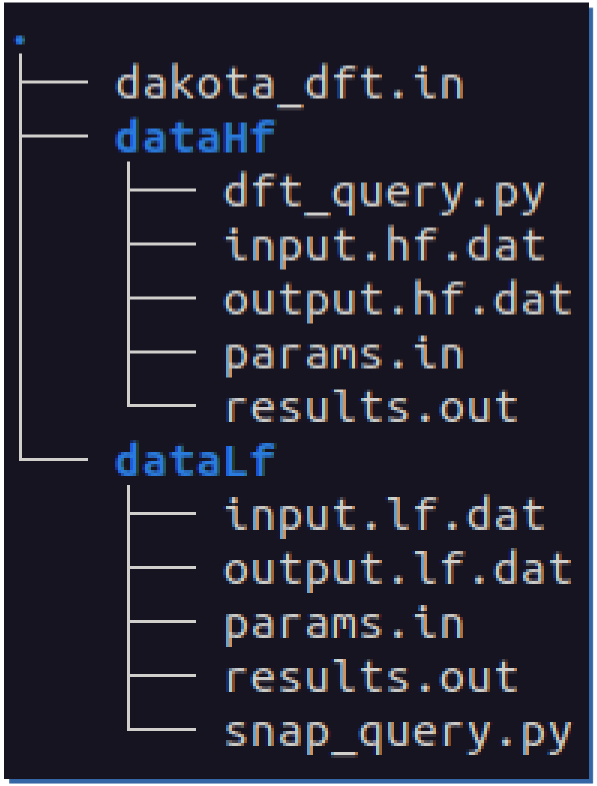

```
.
├── dakota_dft.in
├── dataHf
│   ├── dft_query.py
│   ├── input.hf.dat
│   ├── output.hf.dat
│   ├── params.in
│   └── results.out
└── dataLf
    ├── input.lf.dat
    ├── output.lf.dat
    ├── params.in
    ├── results.out
    └── snap_query.py
```

Results: GP-MF model

- Convergence of the Multi-Fidelity Gaussian Process (MFGP) model with respect to the HF data, and with an increasing percentage of the training set (bulk modulus values).

LF vs HF

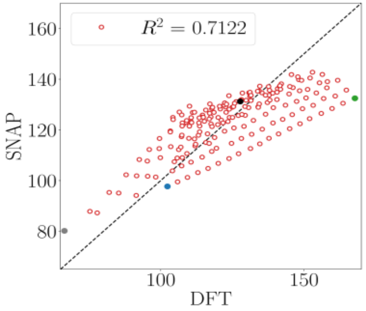

MFGP (10%) vs HF

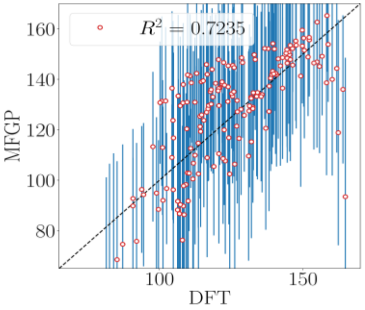

MFGP (50%) vs HF

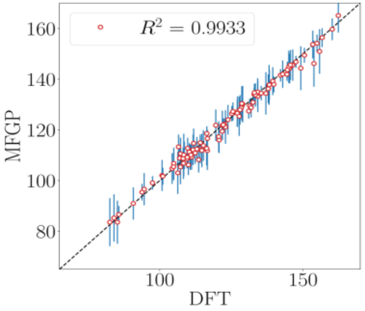

MFGP (90%) vs HF

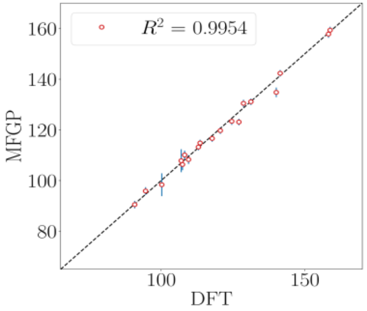

- MFGP vs HF bulk modulus diagram:

HF bulk modulus predictions

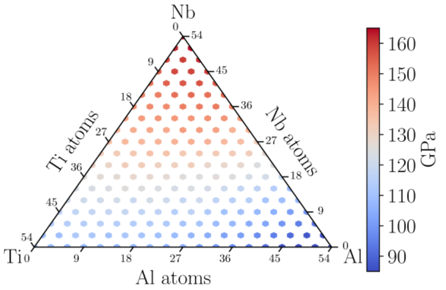

MFGP bulk modulus predictions

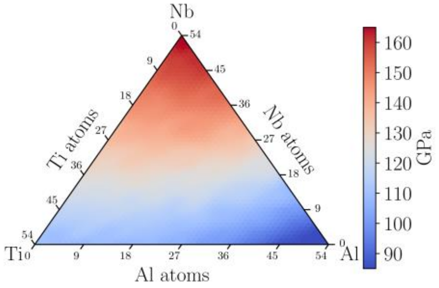

Results: MF Bayesian optimization

- We performed a multi-fidelity Bayesian Optimization (MFBO) research of the optimum bulk modulus value across the AlNbTi composition space diagram:

MFBO: Iteration 5

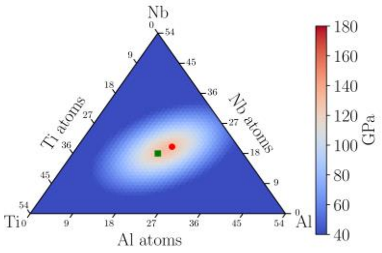

MFBO: Iteration 25

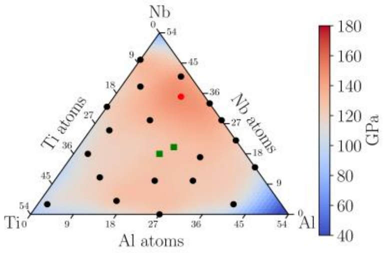

● LF evaluation

🟩 HF evaluation

🔴 Best HF point so far

MFBO: Iteration 36

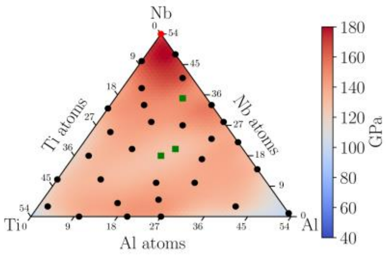

- The optimum bulk modulus value is located at iteration 36, after only 4 expensive HF evaluations.

MFBO: Iteration 131

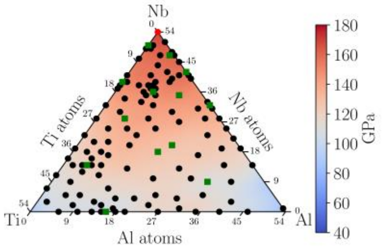
Nb
Ti
Al
Ti atoms
Nb atoms
Al atoms
GPa